Chapter 5

Multi-resolution Feature Extraction and Visual Scene Segmentation of Primate Visual Cortex

5.1 Introduction

Previous studies have found ample evidences of robust computational capabilities of neuron morphologies. Unique morphologies of neurons are tuned to specific frequency of inputs extracting specific information. Specific morphologies in visual cortex are connected with precise connectome specificity, shaping global response in the primary visual cortex. But very little has been understood about the role of electrophysiology and morphologies of dendritic arbour in shaping such complex responses. The size of the RF and spatial resolution is suspected to dependent on the dendritic spread. A midget ganglion cell, with a small dendritic spread is capable of extracting fine local feature whereas a parasol cell with a larger RF focuses on the coarser features. The electrophysiological basis of such behavior remained unexplored till date. Most of the neural network studies focuses on the mathematical interpretation of global behavior rather than local dynamics shaping global responses and defines such networks as learning systems. Basic operations such as edge detection, scene segmentation, multi-resolution feature extraction, depth perception, and motion estimation etc. computed in the striate cortex of primate vision are hypothesized as inherent behavior rather than an exhaustive

learning process. A diverse collection of neuron morphology is believed to play a key role in the process of these basic visual operations.

An attempt has been made in this work to bridge the link between parasol cell and midget cell physiology, nonlinear dynamics and connectome specificity to multi-resolution feature extraction in primary visual cortex. Multiple morphologically detailed midget and parasol RGCs has been designed and modeled to simulate their local behavior integrating active and passive membrane dynamics. Peculiar arrangement of midget and parasol RGCs forming RGC layers has been constructed as prescribed in the in-vivo experimentation to mimic the global responses in these layers.

5.2 Related Works

Morphological segregation and classification of neuronal cells has been conducted since the landmark work of Ramon y Chajal to discover functional significance of unique neuron morphologies. Parasol cell and midget cell morphologies projecting information to magnocellular and parvocellular layers in visual cortex via dedicated parallel pathways has long been established [248–250]. A major challenges in understanding the organization and function of parallel visual pathways is to identify the structural and functional links between the component neurons at successive stages in the path [102, 251–253]. Development in intracellular recording [254–256] and staining methods [248, 257] has emerges to further understand the structure-function relationship but limited to structurally and functionally uniform neuronal layers. Later intracellular recording with tracer injected to magnocellular and parvocellular layers successfully linked functional attributes to anatomical cell types in the retina based on morphology of RGC. Findings points out that the midget ganglion cells with small dendritic spread, connected to red and green cone cells responsible for extracting fine features, projects to parvocellular layer [258, 259]. On the other hand parasol cells which are larger in size with complex dendritic arbor and larger dendritic fields are responsible for contour detection, object detection, boundary estimation and motion perception, projected onto the magnocellular region [248, 249, 260, 261]. Literature confirms midget cells to have higher spatial frequency, low contrast sensitivity, carrying color opponent signals contrary to parasol cells low frequency selectivity and high contrast sensitivity [262–267]. High frequency selectivity and color opponent signal with ON and OFF connectivity with small dendritic spread confirms fine feature detection in midget ganglion cells responsible for pattern recognition and identification. On

the other hand, low spatial frequency selectivity along with contrast sensitivity and larger RFs infers coarser features such as object boundary and contour like features segregation for object detection, object tracking and motion estimation. But structure-function relationship and role of types of non-linearities in shaping complex neuronal responses is poorly understood.

5.2.1 Approach

The objective of this chapter is to mathematically model and replicate responses of parasol and midget RGC neuro-dynamics. Considering different spatial spread of dendritic arbour, their connection specificity along with active dendritic integration discussed in literature. Population responses of the modelled RGC morphology mimicking local responses of midget and parasol RGC layers is explored. Role of sympathetic as well as antagonistic connectivity of RGCs in computing different feature space will also be investigated. Function-structure relationship remained unexplored due to the sizes of midget and parasol cell structures and unavailability of measuring devices to map such relationships to unique morphology. Therefore, availability of a detailed computational model provides insight into the micro and macro process associated in shaping function specific computation in cellular levels.

5.2.2 Contribution

The model simulation responses gives a clear understanding of the role of different sizes of RFs. The simulated model of the midgit and parasol RGC networks, which is supported by the literature, strongly suggests their sensitivity to finer to coarser feature extraction reliance. The response of the midget and parasol cell toward finer and coarser features respectively and their projection onto parvocellular and magnocellular regions give a good idea about the role of fine and coarse feature in either object identification or motion estimation.

5.3 Multi-resolution Model Architecture

Considering the existing in-vivo as well as in-silico literature, an attempt has been made to replicate striate cortex RGC layer arrangements to get a vivid understanding of the local processes associated with visual perception. Emphasis

has been given to detailed morphology of midget and parasol RGCs that can be found making connections with as low as bipolar cells (BC). These midget and parasol RGCs extract complex features from the visual scene, projecting important features to mutually exlusive pervocellular and magnocellular layers that later helps in learning and shaping complex cognitive behavior.

In this work, exclusive morphologies representing midgit and parasol RGCs has been modeled with dendritic arborization as well as active and passive membrane dynamics to the cell. Modeled RGCs are arranged in precise repetitive manner making connections with BC. Layers of RGC morphologies with analogous biophysics are responsible for homogeneous feature extraction and feed-forwarded to successive layers. Special attention has been given to orientation-selectivity and segmentation type behavior in primates striate cortex [249, 252, 268, 269] and their relevance to the type of connectivity with BCs and RGC morphology. Appropriateness of active integration at localized regions of RGC has also been explored in this proposed framework. Details of the model implementation is discussed in the subsequent subsections.

5.3.1 Midget and Parasol Cells

One of the major discovery about organization of retina was the several classes of RGCs, precisely organised with single cell precision to collect information and project onto specific layers. In mammalians, these cells are categorized into two major classes known as midget ganglion cells with smaller dendritic spread and parasol cells with complex dendritic arbor accommodating larger dendritic spread. These cells are identified using staining procedure as well as high resolution imaging describing their unique morphological and anatomical features. Midget cells are described as cells with smaller cell bodies and small dendritic arbors contrary to the parasol systems, having a comparatively larger cell body, complex dendritic arborization with approximately 3 times the dendritic spread of a midget system [265, 270–272]. In-depth study from single cell anatomy recordings portrays a vivid description of the parasol and midget cell system with both the variant having ON and OFF sub-variant antagonistic center/surround organization [273–275]. Literature confirms the rise of midget and parasol cell systems from as low as the bipolar layers making direct connections to the rod and cone photo receptors [276–279]. With a small dendritic spread, the midget cell system connects to limited BCs within a region giving rise to smaller RFs contrary to the parasol system where the dendritic spread stretches across multiple cells over larger regions con-

structing larger RFs. Although the photo receptors form a single layer, multiple connections with ganglion cells gives rise to interesting arrangements of multitude of overlapping RFs [268, 280, 281]. Though the overall functional contribution of such layers are well explored, the computational aspect of individual neuron remained unmapped. Similar neuronal attributes with modification in dendrite arborisation and connectome specifics significantly changing the overall behavior of a network is pronounce. The macro association of functional behavior with respect to the anatomical dynamics is not well understood/overlooked.

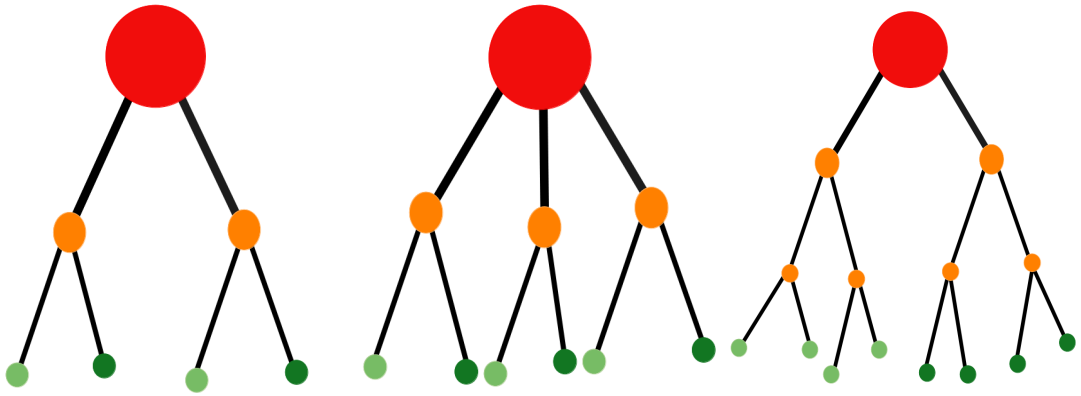

(a) Midget RGC morphology 1. **(b)** Midget RGC morphology 2. **(c)** Parasol RGC morphology.

Figure 5-1: Morphologycally detailed midget and parasol RGCs used in the simulation model.

Shown in Figure5-1 are the detailed morphology integrated to the proposed multi-resolution feature extraction framework where Figure5-1a corresponds to a midget RGC with very small RF with four distal dendritic inputs, Figure5-1b corresponds to another midget RGC with comparatively larger RF with three parent dendrites and six daughter dendrites branching from the parent dendrites. Similarly Figure5-1c has been constructed with multiple layers of dendritic arborization, mimicking a simple parasol RGC. The distal dendritic tips are connected to BCs that in turn processes the incoming signals to extract meaningful information and features that are forwarded to the successive layers for learning and cognition.

An attempt has been made to model morphologically detailed RGCs representing midget and parasol RGCs to explore their computational functionality in the primary visual cortex. Detailed RGCs are designed considering their dendritic arborization, passive fiber dynamics and localized non-linear integration due to differential distribution of AIC. Modeled similar RGCs are connected to grids of photo receptor cells via the BCs to form layers of midget and parasol RGC layers and explore their probable role in feature extraction. To mimic the dendritic

spread of midget and parasol cells, grid sizes of 3×3 and 5×5, 7×7 respectively has been taken for system modeling.

5.3.2 Connectivity, Receptive Fields Sizes and Resolution

As discussed in the literature, midget and parasol cell connectivity can be seen rising from as low as BCs with ON and OFF type sub-variants. Connectivity of midget and parasol cells with BCs form mosaic patterns giving rise to interesting regular arrangements. These arrangements spreads across small regions to larger neighbourhood giving rise to multitude of overlapping RFs within the same layer as shown in Figure5-2 and similar RFs for multiple orientation selectivity as shown in Figure5-2a and Figure5-2b might intermingle to form much complex overlaping RFs. These connections may vary solely from ON/OFF BCs as well as combinations of ON-OFF BCs. Such connectivity patterns forms the basis of RFs. These RGC RFs' size varies depending on the dendritic spread over the neighbourhood of the BCs. The overall response of a neuron might vary significantly corresponding to the RGC's dendritic spread or the type of connectivity with BC.

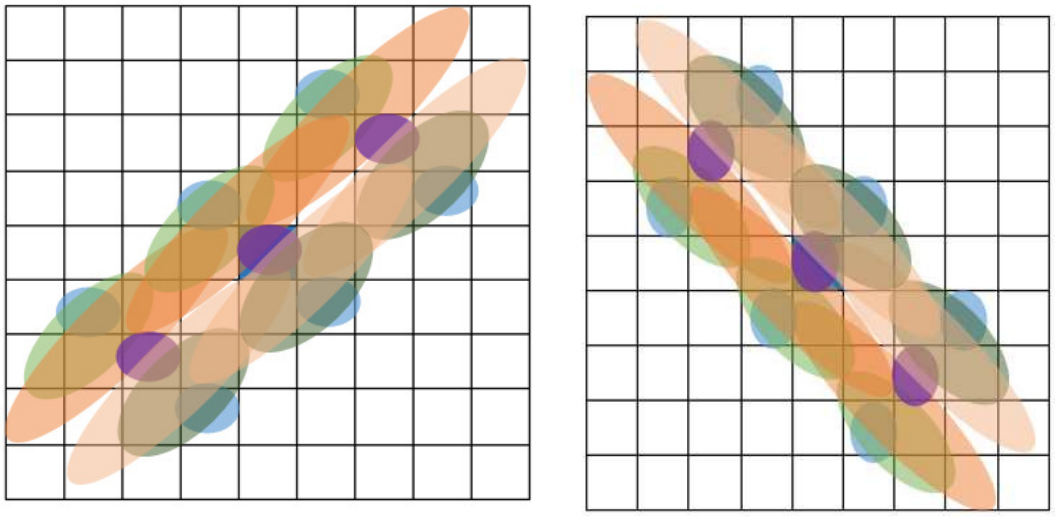

(a) Overlapping RFs of different sizes for orientation selective RGC connections for edge detection at an orientation selectivity of 45°.

(b) Overlapping RFs of different sizes for orientation selective RGC connections for edge detection at an orientation selectivity of 135°.

Figure 5-2: Overlaping RF formation due to orientation selectivity type configuration.

Ovals in different colors in Figure5-2 are the connectivity pattern representation of neurons corresponding to sympathetic/ antagonist connections with BCs

corresponding to RF formation depicted by oval shapes of different sizes. Different sizes of RFs shows dendritic spread of parasol or midget cells within the neighbourhood of BCs. Ovals of same sizes with light and dark color representation suggests connectivity with same parasol/midget cells with antagonist or protagonist BC connectivity. Larger the size of the cell, larger is its dendritic spread and larger is the RF and vice versa. But resolution of RGC operation is confined to the dendritic spread of a cell. Smaller the dendritic spread of a neuronal cell, the associated cell processes information within the local region and thus higher is the spatial resolution of the cell whereas large the dendritic spread, the cell processes information within the larger neighbourhood considers the overall response due to the neighbourhood stimulus and lower is spatial resolution.

The connectivity of RGC in the designed model is associated with the BC. Exclusive connections of RGCs with ON bipolar or OFF BC as well as combinatorial connections of ON and OFF BCs with RGC has been explored in the proposed frame work. Connectivity of RGC's with BCs are represented by matrices, representing the neighborhood of interest. A non-zero value in the connectivity matrix represent connectivity of RGC with BC at corresponding spatial location, whereas a zero value in the connectivity matrix represents no connectivity as shown in Figure5-3.

Apart from zero and non-zero values in the RGC connectivity configurations, '1' and '-1' values has been assigned to represent the type of connectivity with sub-variant of BC as shown in Figure5-3. A value of '1' in the connectivity matrix suggests an excitatory connection with a ON BC whereas a value of '-1' suggests an inhibitory connectivity with BCs. Figure5-3a, Figure5-3b and Figure5-3c shows connectivity matrix corresponding to midget and parasol RGC to BC along with RF interpretation due to their connectivity. Sizes of RFs can be visualised from the pictorial representation of the modeled system where connectivity configuration in Figure5-3a displays a small RF where as RFs in Figure5-3b and Figure5-3c are comparatively moderate and large sizes respectively corresponding to dendritic spread within a bipolar neighborhood of 3×3 and 5×5 cells. In case of a smaller RF, the connected RGC collects and processes information within a small neighborhood empowering the RGC to extract information at a higher resolution. Contrasting to smaller RFs, a RGC connected to larger RF as shown in Figure5-3c, extracts feature from a wider neighborhood resulting in overall information from the neighborhood, thereby reducing the spatial resolution. The RF neighbourhood can be much larger than the interpretation shown in Figure5-3 and the model implementation has been incorporated to understand the effect of

dendritic spread on spatial resolution considering the computational complexity of the system.

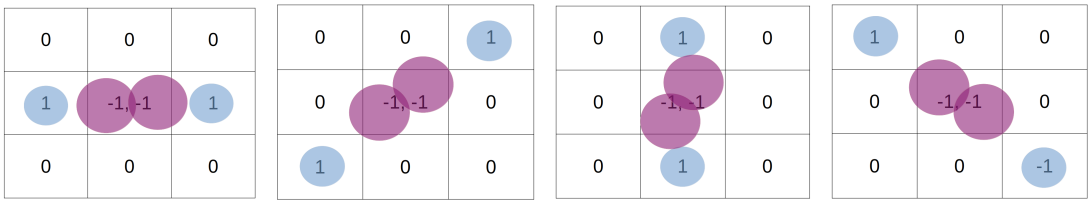

(a) Midget RGC on-phase connectivity over a 3×3 grid for single cell size RF.

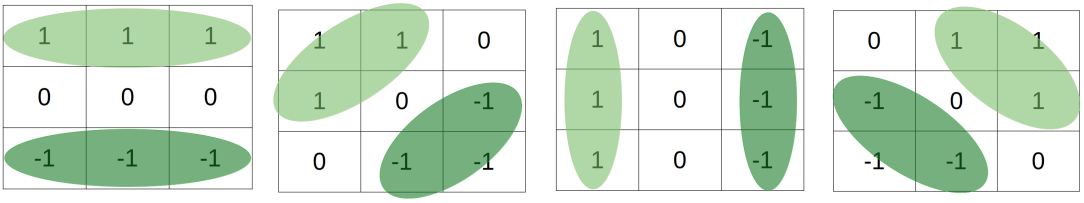

(b) Midget RGC on-phase connectivity over a 3×3 grid for a moderate size RF spreading over three BCs.

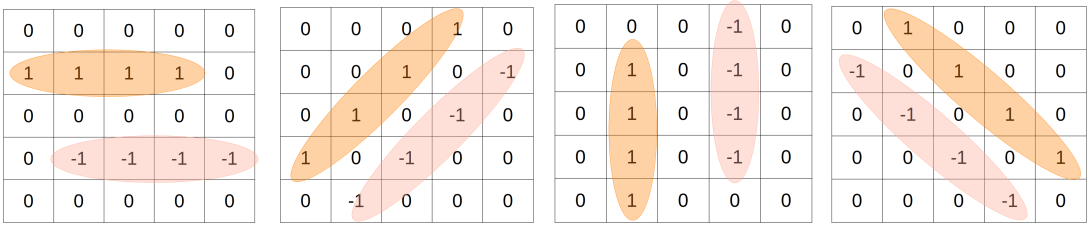

(c) Parasol RGC on-phase connectivity over a 5×5 grid for a comparatively larger RF spreading over BCs.

Figure 5-3: Connectivity matrices corresponding to midget and parasol cell connections with BCs forming RFs shown in Figure5-2 of different sizes respective to their dendritic spread.

5.3.3 Orientation-Selectivity, Dendritic Spread & Spike Triggers

The modelled RGCs corresponding to midget and parasol cells has been integrated to the Orientation selective RGC layer model discussed in the previous chapter. Orientation selective RGC model is particularly associated with orientation specific feature extraction that in turn shapes edge and texture extraction. These features are closely associated with pattern classification, object recognition and identification behaviors in primates. Similar RGC morphology with localized non-linear integration at junctions and nodes has been used (refer 4.3.2.1). Contrary to single RF size in the Orientation selective RGC layer model, the work discussed in this chapter concentrates on different RF sizes to understand the consequences of larger RFs on oriented feature extraction. A BC neighborhood of 3×3 grid

for midget and 5×5, 7×7 grids for parasol RGC dendritic spread has been used. Connectivity matrix for midget RGC within a 3×3 grid of BC is as shown in Figure5-3b that are directly or indirectly stimulated by the photoreceptors. In midget RGC layer model, dendritic spread of one cell has been taken to mimic a midget RGC neighbourhood. Input to the model are grayscale natural images in 'png', 'tiff' and 'jpeg' formats where each pixel represents stimulus to single photoreceptor cell. Configuration and behaviour of the BCs are discussed in detail in the section 4.3.1.2. When the midget network is stimulated with inputs, the RGCs associated to the network extracts oriented features with $\pm 45°$ error which has been seen in simulation results discussed in section 4.4.1 and orientation histogram comparisons in 4.5.4. Respective spike triggers for the RGC has been shown in Figure5-4.

(a) Spike trigger for midget RGC layer configure at 0° orientation selectivity.

(b) Spike trigger for midget RGC layer configure at 45° orientation selectivity.

(c) Spike trigger for midget RGC layer configure at 90° orientation selectivity.

(d) Spike trigger for midget RGC layer configure at 135° orientation selectivity.

Figure 5-4: Spike trigger for midget RGC layer with dendritic spread over 3×3 spatial grids for different orientation selectivity configurations.

Spike triggers for the midget RGC network also shows the orientation selectivity error and the results from a complete oriented edge map as well as spike trigger shows similar redundancy. The error in orientation selectivity of the midget RGC network is primarily due to the nature of oriented information as well as size of the RF. Smaller is the RF higher is the sensitivity of connected RGC that in turn results in higher orientation-specific feature detection error.

The above simulation has been repeated with exactly same inputs and BC configuration but replacing the midget RGC morphology with a parasol RGC shown in Figure5-1c and connection specificity shown in Figure5-3c. The electrophysiology of the parasol RGC is exactly similar to the midget RGC with localized AICs in specific regions such as distal dendritic tip, dendritic junction and the cell

body but the dendritic spread of the parasol RGC spreads over a bipolar grid of 5×5. Stimulating the configuration with inputs generates responses with spike triggers as shown in Figure5-5. On the other hand, repeating the same experimentation with a dendritic spread of 7×7 bipolar grid, spike triggers yield are shown in Figure5-6.

(a) Spike trigger for parasol RGC layer configure at 0° orientation selectivity.

(b) Spike trigger for parasol RGC layer configure at 45° orientation selectivity.

(c) Spike trigger for parasol RGC layer configure at 90° orientation selectivity.

(d) Spike trigger for parasol RGC layer configure at 135° orientation selectivity.

Figure 5-5: Spike trigger for parasol RGC layer with dendritic spread over 5×5 spatial grids for different orientation selectivity configurations.

(a) Spike trigger for parasol RGC layer configure at 0° orientation selectivity.

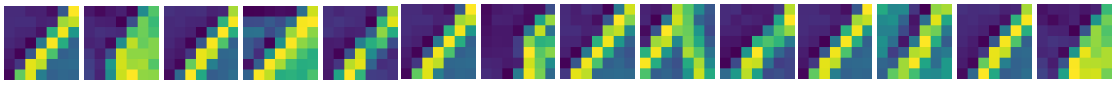

(b) Spike trigger for parasol RGC layer configure at 45° orientation selectivity.

(c) Spike trigger for parasol RGC layer configure at 90° orientation selectivity.

(d) Spike trigger for parasol RGC layer configure at 135° orientation selectivity.

Figure 5-6: Spike trigger for parasol RGC layer with dendritic spread over 7×7 spatial grids for different orientation selectivity configurations.

Comparing the spike triggers in Figure5-4, Figure5-5 and Figure5-6 specific to orientation selectivity, it can be seen that the accuracy of orientation selectivity improves significantly. Considering the spike triggers it can be inferred that the RGC becomes more selective to coarser oriented features with an increase in dendritic spread whereas the midget RGCs are susceptible to fine features as well as coarse features. Further to validate the accuracy improvement of larger RF over

smaller RF, an oriented feature histogram for the three RFs 3×3, 5×5 and 7×7 corresponding to midget RGC and parasol RGC has been compared and shown in Figure5-7. To compute the orientation specificity of the midget and parasol RGCs HOG features from the input image have been calculated and extracting the phase angle information at every point of the input image. The phase angle map due to gradient change is then convoluted with the RGC-specific binary information extracted by the orientation-selective RGC layer. The process of convoluting the orientation-selective RGC responses to the total phase map gives the phase angles at the locations of extracted oriented features. The phase angle information in the convoluted response is represented as a polar histogram to describe orientation selectivity specificity. Detail of the process is shown in Figure4-21 in section 4.5.3.

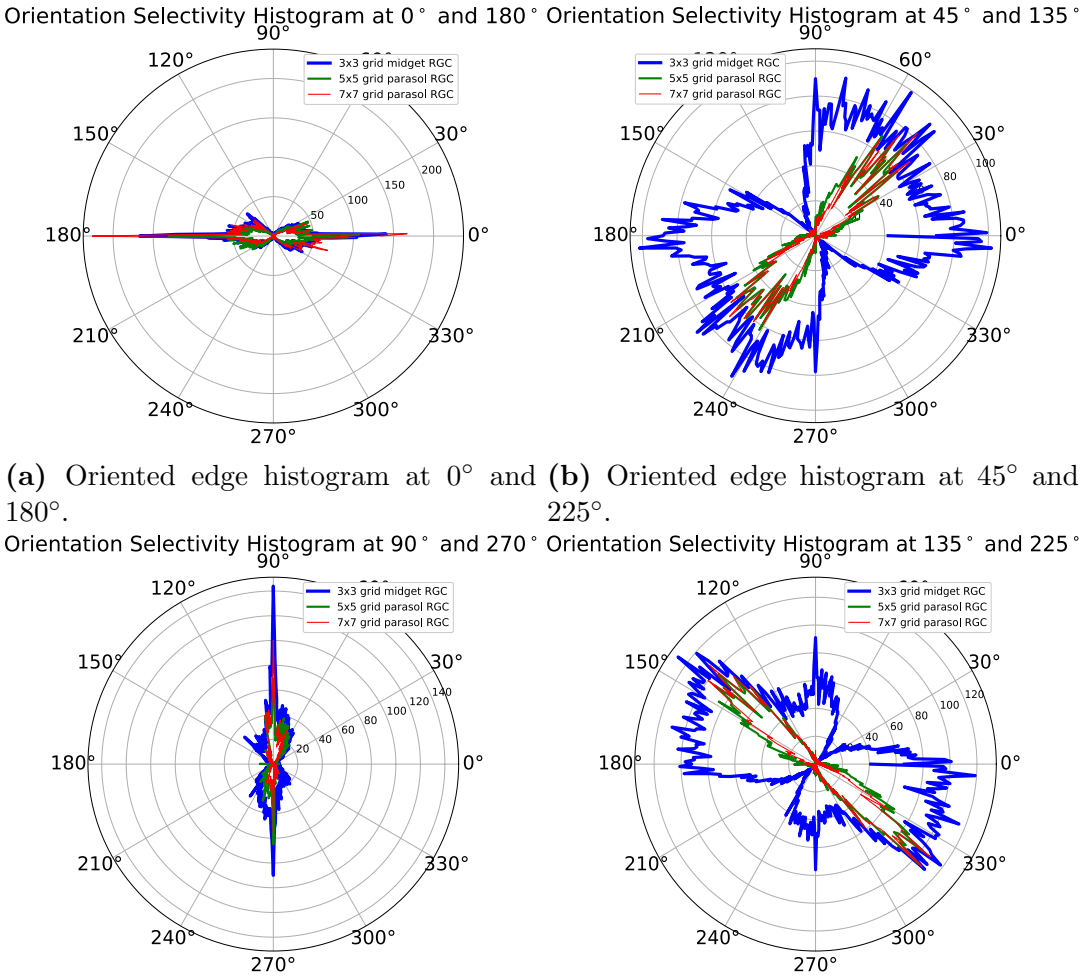

(a) Oriented edge histogram at 0° and 180°.

(b) Oriented edge histogram at 45° and 225°.

(c) Oriented edge histogram at 90° and 270°.

(d) Oriented edge histogram at 135° and 315°.

Figure 5-7: Orientation selectivity histogram showing specificity of different RGCs within grid sizes of 3×3 neighbourhood for midget RGC and 5×5, 7×7 neighbourhood of parasol RGCs.

Shown in Figure5-7a, Figure5-7b, Figure5-7c and Figure5-7d are the oriented edges and texture histogram extracted by orientation-selective RGCs. The

(a) Sample input image from BSDS500. **(b)** Edge map for 3× 3 grid RF. **(c)** Edge map for 5× 5 grid RF. **(d)** Edge map for 7× 7 grid RF.

Figure 5-8: Edge map reconstructed from input image in Figure5-8a by the orientation selective RGC network corresponding to different RF sizes.

histogram shows the bandwidth of orientation selectivity is much wider in midget RGCs as compared to parasol RGCs. As the RF sizes increase, the orientation-selective RGCs are much more precisely tuned to their respective oriented features compared to their smaller counterparts. Their bandwidth behavior corresponding to RF suggests multi-resolution nature where smaller RFs are susceptible to fine as well as coarse features whereas larger RFs are sensitive toward coarser features.

5.3.4 Simulation Results

The described model is implemented using the interpreter 'Python 3.6'. Basic image manipulations are performed with the 'open CV' and 'scikit' libraries, and system of differential equations are computed with 'scipy.integrate' module. Natural images in 'tif', 'png' and 'jpg' are fed as inputs to the model. These natural images are collected from the Berkeley segmentation database (BSDS500) consisting of natural images. When these inputs are fed to the designed model, orientation selective RGC layers extracts oriented features corresponding to 0°, 45°, 90° and 135° orientation features in two opposite phases. Multiple stack of oriented feature at ON-phase and OFF-phase are collected and max pool operation has been performed at every spatial location to reconstruct the complete edge map.

Shown in Figure5-8a is the sample input and corresponding responses of orientation selective RGC network with RF sizes of 3×3 Figure5-8b, 5×5 Figure5-8c and 7×7 Figure5-8d grids. Responses of midget and parasol RGC network corresponding to a RF is constructed from the two complementary phase 0°, 45°, 90° and 135° orientation selective responses and shown in Figure5-8b whereas

larger RF within a grid size of 5×5 and 7×7 are shown in Figure5-8c and Figure5-8d respectively. The ON phase and OFF phase responses of the sample inputs are also shown in Table.5.1. Comparison of 3×3, 5×5 and 7×7 RF responses shows clear indications of smaller RF networks being susceptible to fine as well as coarser features whereas the larger RF networks being inclined more toward much coarser features.

Table 5.1: Orientation selective ON RGC layer response at 0°, 45°, 90° and 135° orientation and OFF RGC layer response at 0°, 45°, 90° and 135° orientation in scotopic vision corresponding to sample images in Figure5-8 respectively.

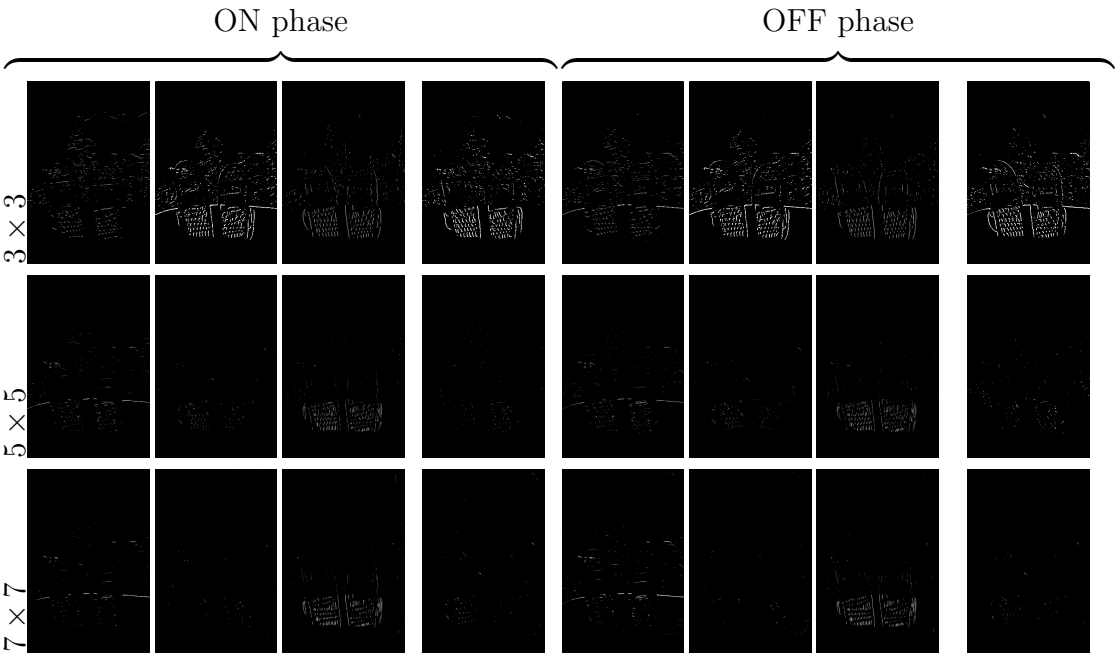

Response of midget and parasol RGC networks shows consistency with respect to their selectivity of oriented features as seen in Table.5.1. Orientation selective midget RGCs connected within a RF size of 3×3 grid picks up fine textures of the tree, forests and mountains whereas RGCs connected to larger field of 5×5 and 7×7 extracts boundaries of the objects within the scene. Detection oriented elements in the larger RF generated edge map are significantly lower as compared to the larger RF counterpart which is due to their sensitivity toward coarser features. On the other hand smaller RFs are sensitive to fine features as well as coarse feature and results in larger detection element density. Detected element density of RFs are also susceptible to amount of oriented feature contents in the input. More finer/coarser feature in input results in more oriented features and vice versa. In case of inputs with mostly homogeneous regions results in sharp bandwidth tuning whereas inputs with multiple objects and non-homogeneous regions results in broader oriented bandwidth. Similar responses can be seen in some of the input responses presented in Figure5-9.

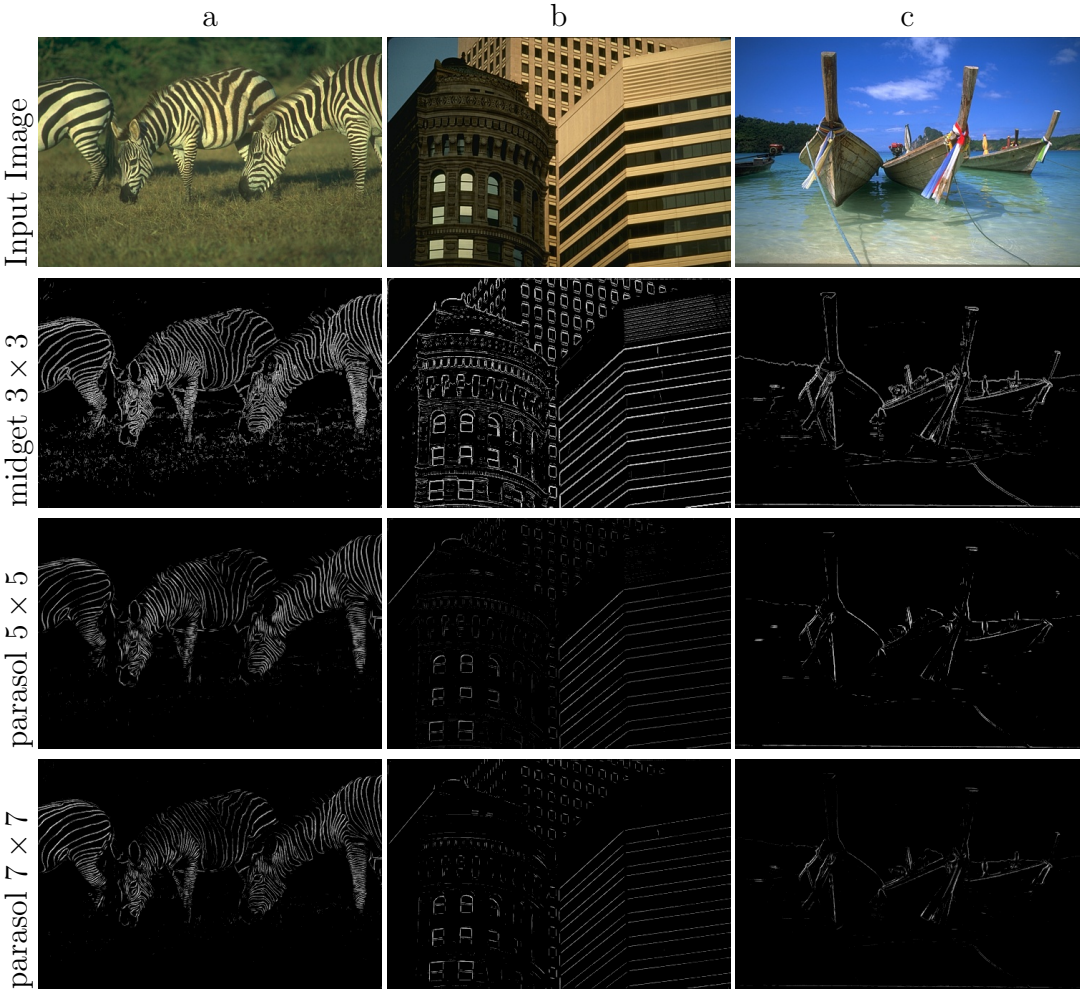

Figure 5-9: Edge map constructed from orientation selective midget and parasol RGC layers corresponding to three different RF sizes showing multi-resolution behavior with midget RGCs replicating high resolution texture as well as boundary estimation and larger RFs extracting coarser boundary maps.

In case of input image shown in Figure5-9(a), the natural image contains multiple 'zebra' with a blurred background and fine grass textures. The midget RGC network with 3×3 RF, being sensitive to fine as well as coarse features, picks up fine features of grass as well as shadows of 'zebras' along with coarse black and white strips and boundaries of the zebra. But looking into the responses of parasol cell with 5×5 and 7×7 RF sizes, they fails to detect fine textures of grass but at the same time it extracts accurate information about the stripes, their boundaries and traces of their shadows. Similar responses can be seen in Figure5-9(b) and (c) responses.

5.4 Segmentation & Boundary Estimation Framework

Primate visual cortex consists of collections of unique RGC morphology arranged in patterns to extract meaningful information from the input. Small neurons with moderate dendritic arborization spreading over small regions called as the midget cells, projects to the parvocellular region via parallel pathways. On the other hand neurons with larger dendritic field and arborization connects to bipolar region over a larger spatial neighborhood projects the extracted information to the magnocellular region. These two regions are isolated from each other and suspected to play important role in visual functions. Parvocellular region contains information corresponding to smaller RFs processed by midget RGCs such as fine textures, complex edge information and features that plays an important role in pattern recognition and identification. Contrary to the parvocellular region, the magnocellular region contains information from parasol cell forming larger RFs such as object boundary and contours that plays an important role in object detection, object tracking and motion estimation. Connectome specificity of RGCs with antagonist BC configuration reveals the high pass filtering nature. Midget cells with complementary BC results in edge and texture feature extraction whereas parasol cell under similar consideration extracts coarser edges. But apart from RGCs connections with complementary BCs, connectivity with only ON-BCs or only OFF bipolar has also been reported and functional significance of such connectivity configuration is yet to be explored.

5.4.1 Model Architecture

The morphology of parasol cells and midget cells that project information to the magnocellular and parvocellular layers of the visual cortex via specialized parallel pathways have long been known [102, 265, 280]. Identifying the anatomical and functional relationships between the component neurons at consecutive points in the path is a crucial problem in understanding the organization and function of parallel visual pathways [282, 283]. Our model employs unique parasol RGCs connected to sympathetic BCs and nonlinear neural electrophysiology in driving scene segmentation functionalities. Natural images in 'tiff,' 'png,' and 'jpg' formats are fed to the model, converted to spatiotemporal square pulses by BCs. A temporal signal with an offset of 10 ms, pulse width of 240 ms, and total temporal length of 350 ms is generated by BCs considering the average response time of primates' vision. The amplitude of the temporal signal is scaled proportionally to the amplitude of signal intensity within the RGC sensitivity range of 1024 nA to 1016 nA. These spatiotemporal signals are fed to the scene segmentation network that generates a segmentation map of the visual stimuli sent to the magnocellular layer. The OS-RGC layer in the magnocellular region then extracts the edge boundary from the segmented image. Details of the RGC morphology and connectome specificity with the BC, as well as boundary estimation in the visual cortex, is discussed in the section 5.4.2 and section 5.4.3 follows.

5.4.2 The Morphology

The proposed framework emphasizes the computational role of unique neuron morphology, particularly parasol RGC, in shaping visual scene segmentation and object boundary estimation. A moderate RF size has been taken [271, 284, 285] to optimize the computational complexity of the model and the morphology is shown in Figure5-10. RGC morphology in Figure5-10a is used for the scene segmentation model, and RGC morphology in Figure5-10b is used for the boundary estimation model where the junctions, cell body synapses, and dendritic fibers are color encoded. The similar color at the synapses suggests the connection of RGC solely with ON-BCs. Junction and soma are modeled as summing nodes that perform temporal summation and re-encoding of cumulative incoming signals. Re-encoding at localized AIC [137, 141] has been modeled using the Izhikevichs'

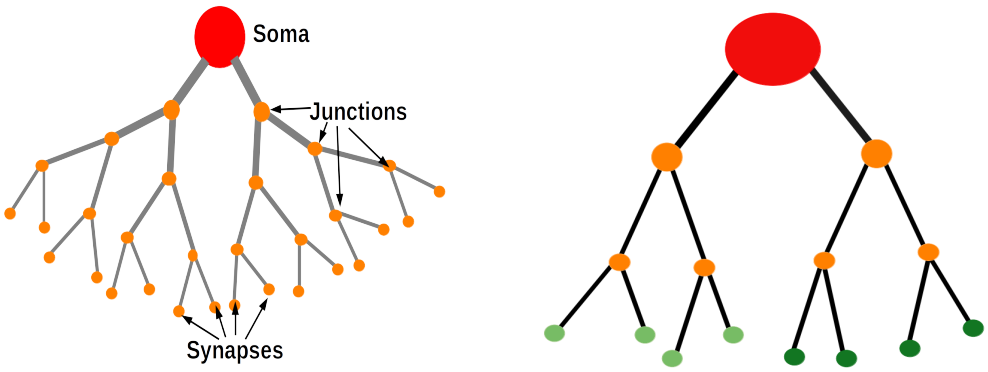

(a) Designed parasol RGC morphology used for scene segmentation.

(b) Designed parasol RGC morphology used for boundary estimation.

Figure 5-10: Parasol RGC morphologies used in striate cortex and magnocellular layer.

membrane model and is given as

$$C\frac{dv}{dt} = k\left((v - v_r)\left(v - v_t\right) - u + I\right), \; if \; v \geq v_t \tag{5.1}$$

$$\frac{du}{dt} = a\left[b\left(v - v_r\right) - u\right], \; v \leftarrow c, u \leftarrow u + d \tag{5.2}$$

where v is the membrane potential with I as the stimuli to the neurons, u as the recovery current, v_r as the resting membrane potential and v_t as the threshold potential. Different spiking activity such as regular spiking, chattering, intrinsic bursting are controlled by parameters a, b, c, d, k, C. Use of Izhikevichs' membrane model [286, 287] in our proposed model is because of its low computational complexity and its robustness in mimicing mammelian neurodynamics. The boundary estimation model employs a combination of 'bursting' and 'chattering' membrane dynamics whereas the segmentation model employs only 'bursting' membrane model.

The passive dendritic branches in the RGC morphology facilitates decremental conduction of propagating signal. Decremental conduction in passive fiber has been modeled using equations

$$I_{inTotal} = I_t + I_{out} \tag{5.3}$$

$$I_{inTotal} = \frac{(V_{out} - V_{in})}{R_{lon}} \tag{5.4}$$

$$I_t + C_m\frac{dV_{out}}{dt} + G_L\left(V_{out} - E_L\right) = 0 \tag{5.5}$$

from the modeling work. V_{in} is the action potential generated by the localized active region, V_{out} is the membrane potential at the junction with initial membrane

0	0	0	0	0
0	1	1	1	1
1	2	2	2	1
1	1	1	1	0
0	1	1	0	0

(a) Gradient normalization at 0°.

0	0	0	1	1
0	0	1	2	1
0	1	2	1	0
1	2	1	0	0
1	1	0	0	0

(b) Gradient normalization at 45°.

0	0	1	1	0
0	1	2	1	0
0	1	2	1	0
0	1	2	1	0
0	1	1	0	0

(c) Gradient normalization at 90°.

1	1	0	0	0
1	2	1	0	0
0	1	2	1	0
0	0	1	2	1
0	0	0	1	1

(d) Gradient normalization at 135°.

Figure 5-11: Parasol RGC connectivity with ON-BCs for normalizing gradient change along specific orientations.

potential equals to resting membrane potential, C_m is the equivalent capacitance of fiber, R_{lon} is the axial resistance, G_L is the membrane leakage conductance E_L is the equilibrium potential due to the leakage ion channels, $I_{inTotal}$ is the total propagating current toward the nodes/ soma, I_t is the transmembrane current due to membrane dynamics, I_{out} is the total delivered current.

5.4.3 Connectome Specificity

Connectome specificity refers to the connectivity of parasol RGC with BCs in the context of the proposed framework. Shown in Figure5-10a are the excitatory type connectivity patterns of RGC morphology Figure5-10a with ON BC which are connected in oriented patterns [186, 288–291]. A value of 1 in the connectivity matrix shown in Figure5-11 corresponds to excitatory connectivity with the ON-BC; the value of 2 in the connectivity matrix suggests two distal dendrites connected to the ON-BC from opposite parent dendrites and value of 0 in the connectivity matrix suggests no connectivity. Scene segmentation type RGC morphologies connected in oriented pattern normalize the small gradient change corresponding to fine features and encode them in terms of their spiking frequency. Four orientation bands that optimize the small local gradient change corresponding to a specific orientation are then passed through the max-pool operator to generate the segmentation type response.

Segmentation type images are then fed to the boundary detection network to extract the boundary information. With the minor gradient corresponding to fine features removed, when the segmented response is passed through the OS-RGC network, the network tracks the primary gradient corresponding to the boundary of objects. The boundary estimation network employs the parasol RGC shown in Figure5-10b with excitatory as well as inhibitory connectivity with specific oriented patterns shown in Figure5-12.

0	-1	0	0	0
-1	-1	-1	-1	0
0	0	0	0	0
0	1	1	1	1
0	0	0	1	0

(a) Orientation selectivity at 0°.

0	0	0	-1	0
0	0	-1	0	1
0	-1	0	1	0
-1	0	1	0	0
0	1	0	0	0

(b) Orientation selectivity at 45°.

0	-1	0	0	0
0	-1	0	1	1
0	-1	0	1	0
0	-1	0	1	0
0	0	0	1	0

(c) Orientation selectivity at 90°.

0	-1	0	0	0
1	0	-1	0	0
0	1	0	-1	0
0	0	1	1	-1
0	0	0	1	0

(d) Orientation selectivity at 135°.

Figure 5-12: Connectivity matrix for boundary detection type RGC shown in Figure5-10b with segmentation type response with orientation specificity to 0°, 45°, 90° and 135°.

A value of 1 in the connectivity matrix suggests excitatory connectivity with RGC, a value of -1 in the connectivity matrix suggests inhibitory connectivity, and 0 suggests no connectivity. These connectivity patterns detect gradient variation corresponding to 1s and -1s and start firing at a high frequency when the gradient is very high.

5.4.4 Simulation Results

The suggested model was simulated using the Python 3.6 interpreter, with packages like 'openCV' and 'scikit' for basic image operations and the 'scipy.integrate' package for solving differential equations. For plotting reaction images and other plot generations, the 'matplotlib' package was utilized in a similar way. Natural images in the 'tif,' 'png,' and 'jpg' formats were used as input to the suggested model, which is employed to stimulate photoreceptor cells, and image data were collected from the Berkeley segmentation database (BSDS500). Shown in Figure5-13 and Figure5-14 are some of the input images fed to the proposed model and their corresponding segmented responses and boundary and contour estimation responses generated by the model.

Shown in Figure5-13 and Figure5-14 (a), (b), (c), (d), (e) and (f) are the input images fed to the BCs that are being encoded into segmented images reconstructed calculating the spiking frequency of the neurons. The RGCs connected to the ON and OFF-BCs encodes the different values corresponding to a neighborhood into spiking frequency depending on illumination strength and homogeneity and in-homogeneity of the region. ON RGC network and OFF RGC networks are complementary to each other both concentration on features in the brighter and darker illumination respectively. Max-pool operation from the two layers gives us the complete 'Segmented Layer' image encoded by the RGC network. These re-

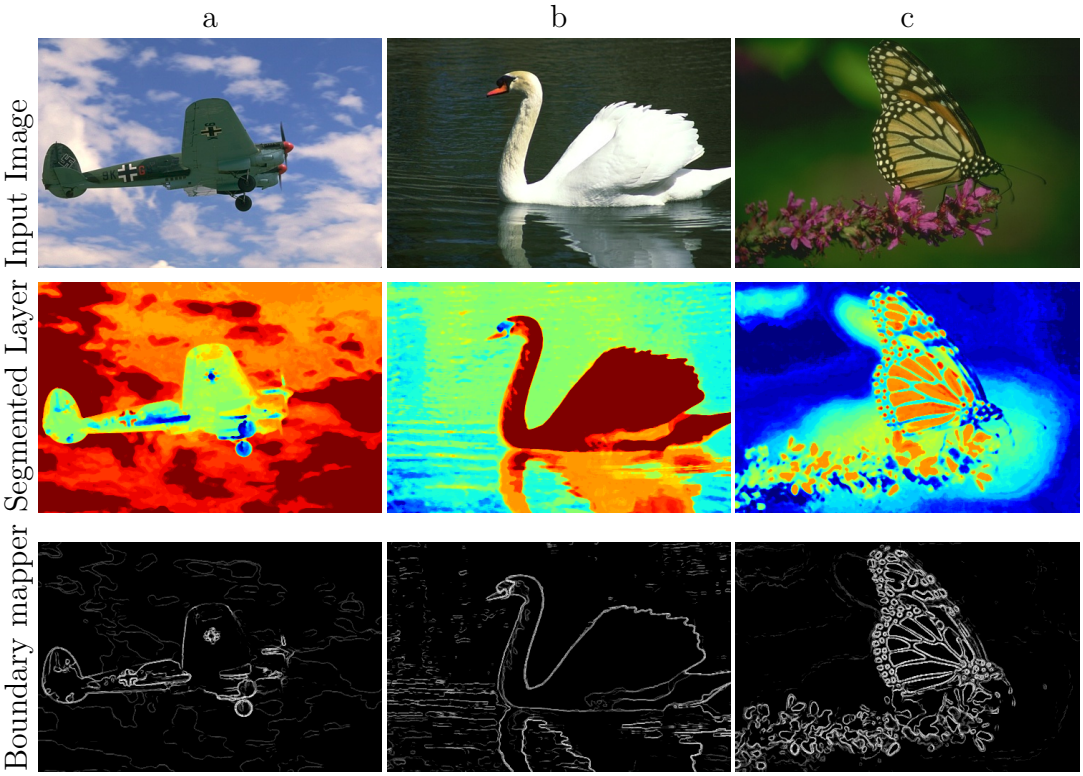

Figure 5-13: Parasol RGC network connected to ON-BC network and OFF-BC network showing segmentation type behavior. Boundary and contour map reconstruction type behavior due to orientation selectivity type network connected to parasol RGC layers with sympathetic connectivity with ON and OFF-BC layer that are being projected onto magnocellular region.

sponses are then fed to OS parasol RGC network that gives the 'Boundary mapper' responses corresponding to the boundary and contour estimation.

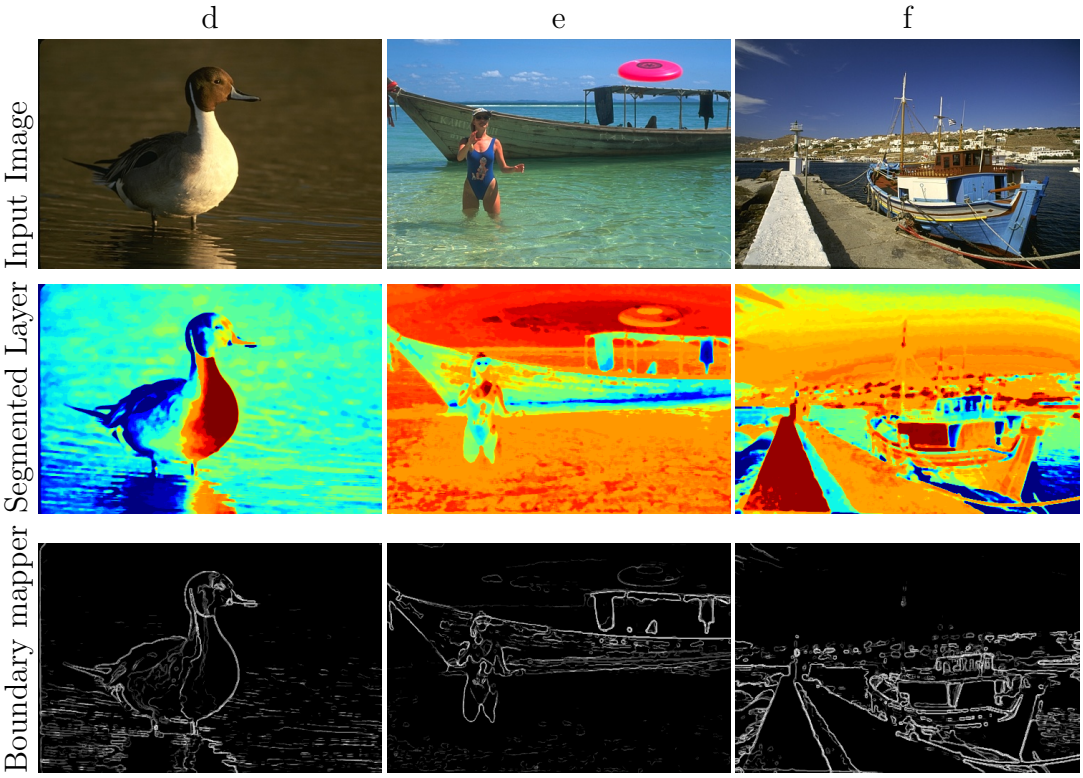

Figure 5-14: Parasol RGC network connected to ON-BC network and OFF-BC network showing segmentation type behavior. Boundary and contour map reconstruction type behavior due to orientation selectivity type network connected to parasol RGC layers with sympathetic connectivity with ON and OFF-BC layer that are being projected onto magnocellular region.

As can be seen from the 'Segmented Layer' response of Figure5-13, Figure5-14 (b) (c) and (d), the model successfully maps most of the boundary regions of the object, whereas responses corresponding to Figure5-13, Figure5-14 (a) (e) and (f) show some texture extraction which is due to the RF size of parasol RGCs in the segmentation layer. Increasing the RF size of the segmentation layer will remove most of the local gradient change making the boundary region more prominent. Thus need for a larger RF projecting to the magnocellular region for better normalization of fine textures seems necessary. However, due to the computational complexity of the model, larger RFs are not being considered and remain to be interset of our future works. Table .4.1 lists the model parameters for modelling the passive membranes' low pass features as well as Izhikevich's membrane dynamics [286, 287]. Izhikevich's membrane model has been included to imitate the behavior of a human's visual cortex due to its capacity to emulate Ca^{2+} ion channel dynamics.

5.5 Summary and Future Remarks

The proposed model gives a clear understanding of the type of feature extracted by parasol RGC networks contrasting to a midget RGC network under a similar model configuration. The model shows midget RGCs susceptibility to fine features whereas parasol RGC networks specificity toward coarser features. Midget and parasol cells form the basis of RF sizes depending on cells' dendritic spread and arborization. When midget and parasol cells are organized with configuration specific to orientation selective RGC layers, show multiresolution feature extraction responses. Midget RGC networks can extract fine features from the scene whereas parasol RGCs with increasing dendritic spread imitates their coarser counterparts. Such features from fine to coarser scales are projected onto the parvocellular region for efficient identification and learning from visual scenes. This work gives a clear understanding of the need for multiple classes of RGCs depending on their dendritic spread within the human visual cortex. The proposed model with parasol RGCs, when connected with only ON-BCs or OFF-BCs with minor connectivity modifications, gives an insight into the conversion of natural scenes in the primary visual cortex layer that later helps form object boundaries and contour. Even though the exact specificity of RGCs connection with other inter neurons is not yet well explored for boundary and contour estimation due to the unavailability of measuring devices, the proposed methodology has been built with reference to in-silico experimentation with connections specifically to either ON or OFF-BCs. These parasol RGC networks connected to BCs processes information corresponding to the size of RF. Connecting the network solely to the ON-type of BCs gives rise to segmentation-type behavior with a relatively moderate RF. The OS-RGC layer connected to segmentation-type responses gives rise to object boundary and contour detection, which is one of the significant features projected onto the magnocellular region of the visual cortex by parasol RGCs. Thus the proposed model gives insight into object boundary estimation, which later helps in complex function formation such as object tracking, object motion, and depth estimation. The proposed multi-resolution can be further implemented in multiple stacks of simple and complex cell learning networks in the parvocellular region to replicate similar responses in primates' visual cortex giving a better perspective of scale and shift invariant learning process. On the other hand, the boundary estimation framework can be used to replicate the magnocellular responses shaping complex function formation such as motion and depth perception in primates.